RSC Advances

ROYAL SOCIETY OF CHEMISTRY

www.rsc.org/advances

RSC Advances

RSCPublishing

ARTICLE

Characterization and properties of organo-montmorillonite modified lignocellulosic fibers and their interaction mechanisms

Ru Liu[a, b], Yu Chen[a], and Jinzhen Cao[a]*

Received 25th June 2015,

www.rsc.org/advances

In this study, lignocellulosic natural fibers (NFs), namely, cellulose fiber/flour (CF) and lignin flour (LF) separated from poplar wood flour (WF) as well as xylan as a representative of hemicellulose flour (HF), were modified with organo-montmorillonite (OMMT) through a two-step method. Some physical and mechanical properties of the thus-modified materials were investigated. Besides, the interaction mechanisms between OMMT and these NFs were studied. The results showed OMMT partly intercalated with HF and completely exfoliated in LF. However, it hardly penetrated into CF. Owing to that OMMT reduced the moisture contents of HF and LF and improved their mechanical properties. But for CF, OMMT showed negative/little effects on its physical/mechanical properties. No reaction was found between OMMT and CF. It mainly reacted with the amorphous constituents of NFs by basically forming on end carboxyl/ phenolic hydroxyl groups of HF/LF molecular chains.

Introduction

The use of renewable natural fibers (NFs) like wood, bamboo, straw, cereal, cotton, hemp, jute, and so on as fillers or reinforcements in composites to reduce the need of fossil products has achieved much attention.[1-3] Compared with conventional inorganic fibers, NF possesses many advantages like abundance, relative low cost, biodegradability, low density, and high specific strength.[4] The NF reinforced composites have been widely used in various applications such as fencing, flooring, decking, railing, and so on in recent years.[5] Although there are thousands types of NF, the primary chemical components of NF are almost the same. They all consist of cellulose, hemicelluloses, and lignin, forming a very complex structure in their cell wall.[6] Cellulose is the main component in a linear polysaccharide form with high regularity and high degree of crystallinity, giving NF its characteristic strength.[7] Hemicelluloses consist of heteropolysaccharides made up of pentoses, hexoses and sugar acids with random and amorphous structure.[8] Lignin is a phenol propane-based amorphous resin that fills the spaces between the polysaccharide fibers, occupying mainly the middle lamella of NF cells and providing shape, structure to the NF.[9] These constituents differ among NF species and affect the physical, mechanical, and thermal properties of the resulting polymer composites.[10]

With the development of nanotechnology, the incorporation of layered silicate nanoclays as *in situ* reinforcements has been intensively investigated on modification of NF products in recent years.[11-14] Owing to the nanoscales of nanoclays, the modified products exhibit dramatic improvements in modulus, strength, gas barrier property, and flame resistance even if the filler amount is small.[15] Besides, nanoclays are also promising enhancer for polymers by increasing the crystallinity, strength and thermal stability.[16-18] Among nanoclays, montmorillonite (MMT) is one of the most widely used types because of its natural abundance and beneficial properties in high cationic exchange capacity, high specific surface area, and large aspect ratio *etc*.[19] The simple chemical composition of layered MMT is $Al_2O_3 \cdot 4SiO_2 \cdot 3H_2O$ and its mean layer thickness is 0.96 nm. To achieve high performance in modified NF composite products, it is essential to completely separate MMT into individual silicate layers.[20] Compared with natural sodium-MMT (Na-MMT), organo-montmorillonite (OMMT) has a better effect on improving the physical and mechanical properties of composites because of its large interlayer distance and compatibility with non-polar polymers.[21] In previous studies,[22, 23] Na-MMT and didecyl dimethyl ammonium chloride (DDAC) were used to modify WF in a two-step impregnation process to form OMMT in-situ, also scanning electron microscope (SEM) and transmission electron microscope (TEM) were used to confirm the existence of OMMT inside the WF. As a result, the properties of the modified WF and its composites with poly (lactic acid) were highly improved.

[a]*MOE Key Laboratory of Wooden Material Science and Application, Beijing Forestry University, Qinghua East Road 35, Haidian 100083, Beijing, China*

[b]*Research Institute of Wood Industry, Chinese Academy of Forestry, Haidian 100091, Beijing, China*

**Correspondence to Jinzhen Cao (caoj@bjfu.edu.cn). Tel/Fax: +86 010 62337381*

As mentioned above, incorporation of OMMT into NF can improve the physical and mechanical properties of NF, which is beneficial for preparing high-performance NF based composites, However, the interaction mechanism of OMMT with NF components is unknown and the properties of OMMT-modified-NF components have not been studied yet. Therefore, this study further investigated the interaction mechanisms between OMMT and NF components, which were helpful to understand the reinforcing mechanism and efficient use of NF. Considering the hemicelluloses flour (HF) were impossible to be completely separated from NF at present, they were replaced by xylan due to the large share of xylan (about 80-90%) in hemicelluloses,[24] while the CF and LF were separated by nitric acid-methanol method and ball-milling coupled with diaxane extraction method from poplar WF, which is a fast growing wood species widely available in northern China. The NF components were modified with OMMT by the same two-step method. The thus-modified NF components were characterized by X-ray diffraction (XRD), Fourier transform infrared spectrum (FTIR), SEM, and TEM analyses. The moisture adsorption, modulus of elasticity, and hardness of the modified and neat NF components were tested. To understand the reaction mechanisms between OMMT and NF components, the ^{13}C solid-state unclear magnetic resonance (^{13}C NMR) analyses was carried out.

Materials and method

Materials

WF of poplar (*Populus tomentasa* Carr.) with mesh size of 40 to 60 was kindly donated by Xingda Wood Flour Company, Gaocheng, China. Xylan, which was used as a representive of HF, was purchased from Nanjing Oddfoni Biological Technology Co., Ltd., Nanjing, China. It is a white powder with average diameter of 38 μm. Na-MMT (PGV; Nanocor Inc, USA) was purchased from market. It is a hydrophilic clay powder with specific gravity of 2.6 and its pH at 5% w/w in distilled water is 9-10. The mean interlayer distance of Na-MMT is 1.417 nm. The cation exchange capacity of Na-MMT is 145 mmol/100 g. The modifier used in this study was DDAC (70%), which was purchased from Shanghai 3D, Bio-chem Co., Ltd., Shanghai, China. The reagents used in this study were all bought from Tianjin Jinke Fine Chemical Institute, China.

Preparation of CF and LF

The CF and LF were prepared according to TAPPI standard[25] and Holtman et al.[26] that used in wood chemistry.

Prior to separation, WF was extracted in a Soxhlet extractor with a mixture of 1:2 ethanol and toluene (v/v) for 6h, followed by a second extraction with ethanol for 4h to remove extractives. The extracted WF was dried in an oven at 103 ± 2 ^{o}C to reach a constant weight. The yield of the extracted WF was about 97%.

The CF was separated as follows: 5g of extracted WF was placed in a 1000-mL beaker, in which 25 mL HNO_3 (68%) and 100 mL of ethanol were added. The mixture was refluxed under shaking in a water bath at 100 ^{o}C for 60 min. After that, samples were filtered using a G2 sand core funnel. The 60-min refluxing cycle was repeated 4 times. Finally, the sample was washed with hot water until reaching neutral pH and then washed with ethanol. The sample was dried at in an oven at 103 ± 2 ^{o}C until the weight was constant. The yield of the CF was about 40%. The average diameter and length of CF were about 62.17 and 500 μm, respectively.

The LF was separated as follows: extracted WF was emerged in toluene and subjected to 48 h of milling at 250 rpm using agate balls by frequency conversion dual planetary ball-mill equipment (Chunlong Instrument SHQM-2L, China). The milled WF was extracted with a mixture of 1,4-dioxane and water (v/v) at a ratio of 9:1. After filtration, the liquor was collected and dried in an oven at 35 ± 2 ^{o}C. The residue obtained was dissolved in a solution of acetic acid and water (9:1, v/v) and then precipitated with water. The precipitated residue was separated by centrifugation. The residue was then dissolved in 1,2-dicloromethane and ethanol (1:2, v/v) and precipitated with diethyl ether to obtain the purified LF. The sample was dried at in an oven at 35 ± 2 ^{o}C to reach a constant weight. The yield of LF was about 8%. The average diameter of LF was about 47.06 μm.

Modification of NF components

The modification process of NF components was carried out on a two-step method as described in previous study.[21] In details, NF components were first placed in a beaker in a treating tank and vacuum-treated at 0.01 MPa for 30 min. Then, 0.5% concentration Na-MMT dispersion was allowed to completely submerge these flours and pressure treated at 0.6 MPa for 1 h. The average particle size of the Na-MMT dispersion was 634.8 nm as determined by Laser Particle Analyzer (Delsa^{TM} Nano C, Beckman coulter, USA). The impregnated materials filtrated and vacuum dried at 60 ± 2 ^{o}C for 24 h. The weight percent gains of these flours were ranging from 0.15-0.35%. In the second step, the treated NF components were placed in a beaker and submerged in DDAC solutions to form OMMT. The concentration of DDAC was calculated according to the concentration of Na-MMT at a ratio of the cation exchange capacity of Na-MMT of 0.7:1, which was 0.26%. The beaker was placed in a water bath at 60 ^{o}C for 2 h with mechanical stirring at a speed of 80 r/min. The modified flours were then filtrated and vacuum dried at 60 ± 2 ^{o}C to constant weight. Compared to the first step, there were additional 3-5% weight gains for NF components.

Characterization of NF components

XRD analysis of the samples was carried out on an X-ray 6000 (Shimadzu, Japan) machine. The X-ray beam was Cu-Kα (λ=0.1540 nm) radiation, operated at 40 kV and 30 mA. The scanning rate was 2 °/s and 2θ ranged from 2° to 40° with the rotational speed of 30 rpm.

The chemical groups of the samples were examined by Fourier transform infrared spectrum analysis spectrometer (FTIR, BRUKER Vertex 70v, Germany), and potassium bromide (KBr) was used to collect the background. Air-dried sample powder, was mixed with KBr in a weight ratio of 1:100 before spectrum collection. All spectra were displayed in wavelengths ranging from 400 to 2000 cm^{-1}.

The morphologies of the samples were observed with a Hitachi (S-3400, Japan) SEM, operating at an acceleration voltage of 5 kV, after sputter-coating with gold.

The sections of the samples were observed in a TEM (JEOL TEM 1010, Japan) for visualizing the distribution of OMMT. Prior to testing, all the samples were embedded in an epoxy resin and cut transversely with an ultra-microtome knife to obtain ultrathin (50 nm) sections.

Moisture adsorption test

All the samples were dried in an oven at 103 ± 2 °C until they reached the constant weight prior to the moisture adsorption test. Four specimens from each unmodified and modified NF components (about 2 ± 0.01 g) were placed in a tinfoil box and then kept in desiccators filled with distilled water at 23 ± 2 °C for 8 days. The weights of the NF components were recorded periodically and the weight percent gains (WPGs) were calculated to denote the moisture adsorption capacity.

Nanoindentation

The nanoindentation tests of NF components were carried out using a Nano Indenter II (MTS Systems Crop., USA) with a diamond tip, as for Xing et al.[27] All the samples were embedded in an epoxy resin prior to testing. The top faces were cross-sectioned and smoothed with a knife, and the specimens were then mounted on an iron plateau. Once the tip contacted the sample surface, a constant strain rate of 0.05 s^{-1} was applied until an indentation depth of 2 μm was reached. The maximum loading force was held for 10 s prior to unloading. A total of 10 indents were made on the samples, and modulus of elasticity and hardness of NF components were obtained.

Interaction mechanism analysis

^{13}C NMR experiments were carried out to further understand the interaction mechanisms between OMMT and NF components by using a 400MHz WB Solid-State NMR spectrometer (Bruker Avance III, Switzerland) at 100.6 MHz. Each dry sample was packed in a 4 mm zirconium oxide rotor. The rotation frequency was 5 kHz. Acquisition was performed with a CP pulse and a 2s delay between repetitions. The temperature was kept at 28 °C.

Results and discussion

XRD analysis

Fig.1a shows the XRD patterns for neat NF components. CF exhibited peaks at 2θ = 17°, 22.5° and 35°, corresponding to a typical crystalline structure of native cellulose I at crystal plane diffraction peaks of (101), (002), and (040), respectively.[28] HF beard a broad peak around 2θ = 20° due to some short-range order in the amorphous polymeric structures.[29] LF showed a very broad peak at 2θ = 5-35°. Thus, it suggested LF was in an amorphous structure.

After treating with Na-MMT, two new peaks appeared in all samples around 2θ = 6° and 19 ° were related to the (001) and (200) plane crystalline structure of MMT (Fig.1b). By calculating from the (001) lattice plane diffraction peak with Bragg's equation, the interlayer distance of MMT could be obtained.[30] The value was 1.417nm which is equal to neat Na-MMT, suggesting the presence of Na-MMT.

After the second modification step, there were some differences in the XRD results (Fig.1c). In samples of OMMT modified CF and HF, peaks shifted to low regions at 2θ = 3.46° and 3.32°, corresponding to the interlayer distances of 2.551 and 2.568 nm, respectively. These values were larger than neat Na-MMT (1.417nm) and DDAC modified Na-MMT (2.323 nm).[21] The enlarged interlayer distance suggested a successful intercalation of DDAC between MMT layers during the second modification process. Accordingly, OMMT was synthesized in CF and HF. Besides, the CF and HF were also positive factors to broaden the MMT layers, suggesting the OMMT underwent partly intercalation with CF and HF. But in OMMT modified LF sample, the two peaks around 2θ = 6° and 19 ° disappeared. Liao and Wu[31] added 7 wt% of clay into WF/Poly (ethylene-octene) elastomer and also found no apparent peak. They suggested that the clay had been fully exfoliated into individual and collapsed silicate layers, thus no regular crystalline structure could be obtained from XRD patterns. Similarly, the OMMT in LF might have completely exfoliated and homogeneously dispersed in LF. This could be expected because LF was the most hydrophobic components in NF and was more compatible with non-polar OMMT than other components. Due to the high crystallinity of CF, OMMT layers were difficult to effectively intercalate with CF. Thus, it exhibited the narrowest interlayer distance. The modification process did not change the crystal structure of CF but affect HF significantly. The magnitude of the broad peak around 2θ = 20° decreased a lot, indicating reactivity of HF during OMMT modification.

FTIR analysis

The FTIR results give evidence to identify the chemical constituents and structures of NF components as well as the existence of OMMT. In Fig.2a, LF did not bear the peak at 1240 cm^{-1} ascribed to C-O ester stretching vibration of hemicelluloses disappeared.[32] For both CF and LF samples, the peak at 1735 cm^{-1} corresponding to ester C=O stretching vibration weakened,[33] indicating the removal of HF. The neat CF and HF did not bear peaks at 1267 cm^{-1} (C-OH stretching of phenolic group), 1460 cm^{-1} (C-H bending of methyl and methylene groups in lignin), 1510 and 1610 cm^{-1} (C=C stretching of aromatic ring skeleton) and 1121 cm^{-1} (aromatic C-H deformation),[34] indicating the absence of lignin. As for LF sample, the cellulose characteristic peaks including C-O-C stretching and asymmetric stretching vibration at 1066 and 1114 cm^{-1}, CH_2 or C-OH vibration at 1312 cm^{-1}, C-H bending at 1371 and 1338 cm^{-1}, and intermolecular –OH bonds bending at 1430cm^{-1},[35] sharply weakened due to the absence of cellulose. Besides, both CF and HF samples retained peaks at 894, 972, 1042, and 1168 cm^{-1}, indicating the presence of β-glycosidic linkages between sugar units.[36] The peak at 1647 cm^{-1} was associated with absorbed water due to the strong water affinity of CF and HF.[32] It should be mentioned that pure xylan contained very a few of ester bonds, therefore, for neat HF sample, the peak at 1735 cm^{-1} was not obvious.[37]

The FTIR results of Na-MMT treated NF components are shown in Fig.2b. Compared with Fig.2a, all the samples remained their own characteristic peaks, indicating the Na-MMT treatment did not influence the main chemical structures of these materials. Besides, two new peaks appeared at 460 and 515 cm^{-1} which were attributed to Al-O-Si and Si-O deformations,[38] indicating the existence of MMT. Also, in OMMT modified LF sample, a peak at 1033 cm^{-1} related to Si-O-Si stretching emerged.[39] However, this peak was overlapped by the C-O-C stretching in Na-MMT treated CF and HF samples. The peak at 1647cm^{-1} sharply increased indicated

more absorbed water in Na-MMT treated samples than the original ones due to the hydrophilic character of Na-MMT.

The FITR results of OMMT modified NF components are shown in Fig.2c. Compared with Fig.2b, the two new peaks at 460 and 515 cm^{-1} remained. Also, in OMMT modified LF sample, a peak at 1033 cm^{-1} still appeared. But the peak at 1647cm^{-1} decreased, suggesting hydrophilic Na-MMT had been transferred to hydrophobic OMMT. The peak at 1735 cm^{-1} was found in HF sample after modifying with OMMT, indicating some -COOH groups formed during HF hydrolyzation, which may be caused by oxidation of $–CH_2OH$ groups.[40]

SEM analysis

The SEM images of neat, Na-MMT and OMMT modified NF components are shown in Fig.3. The structures of the neat materials could be clearly seen from Fig.3a to 3c. For example, the surface of neat CF appeared very clean (Fig.3a). For CF and HF samples containing Na-MMT (Fig.3d-3f), there were some flocculated substances precipitated on the surfaces of CF and HF (see arrow in Fig.3d and 3e), which might be Na-MMT. LF did not show much difference compared with its original appearance. LF has much rougher surface and smaller particle size than CF and HF, which could absorb more MMT on its surface or in the micro-pores. The morphologies of NFs were different, which might affect the impregnation of MMT. After the second modifying, some differences could be observed in CF and HF samples while LF also remained almost the same. The OMMT particles were rarely found attaching on LF surface (Fig.3i), indicating that the intercalated OMMT layers might have evenly distributed into LF matrix. However, as for OMMT modified CF sample, big particles of OMMT were attached on CF (Fig.3g). But it seemed to be separated rather than agglomerated. The HF particles after modifying (Fig.3h) seemed to become more rigid compared with neat HF. Some small protuberances (see arrow in Fig.3h) could be the micro-size OMMT particles encapsulated by HF matrix.

TEM analysis

The high-magnification TEM images illustrate the dispersion and location of OMMT in NF components. From Fig.4a to 4c, the structures of neat CF, HF and LF can be seen clearly.

In both Na-MMT and OMMT modified CF sample (Fig.4d and 4g), great amount of MMT layers stacked with thick MMT agglomerations attaching on the CF surface due to the high crystallinity of CF. Besides, MMT attached on CF embrittled the CF, resulting in breakage of embedding agent of epoxy resin. For HF and LF samples containing Na-MMT (Fig.4e and 4f), Most of Na-MMT layers were not individually separated in HF or LF, but existed in small gathered particles. After modifying with modifier, although some MMT particles could also been found in HF, large amount of intercalated structures of OMMT could be seen (Fig.4h). And for LF sample, it was interesting that OMMT was highly exfoliated in LF (Fig.4i). A single silicate layer has a thickness of 1 nm and an average length of 100 nm.[21] But the length of OMMT in LF was much longer than that value, which could be explained by the hydroxylated edge-edge interaction of the OMMT layers that promoted silicate layer flocculation. The TEM analysis confirmed an assumption that OMMT was interacted with the amorphous constitute in NF cell wall while LF was the main component to exfoliate OMMT.

Moisture adsorption

The moisture adsorption tests for neat, Na-MMT and OMMT modified CF, HF, and LF samples are shown in Fig.5. All samples adsorbed moisture fast at initial and then slowed down to reach a constant. Comparing the moisture contents at each stage and moisture adsorption speed of all samples irrespective of adding MMT, the following order is clear: HF>CF>LF. It was expected since LF was the most hydrophobic component, while HF was the most hydrophilic component. The equilibrium moisture content of CF was lower than HF but little higher than LF. It was known that CF was a kind of hemi-crystal polymer with lots of hydroxyl groups (more than LF). However, in crystal region, the hydroxyl groups were highly bonded with each other, which resulted in less accessed hydroxyl groups to adsorb moisture. The results of moisture adsorption are correlated to the FTIR analyses.

With incorporating of Na-MMT, all NF components showed big improvements in equilibrium moisture contents with values of 16.00%, 53.21%, and 11.29% for CF, HF and LF, which gained about 5%, 3%, and 0.2%, respectively. It was reasonable due to the high hydrophilic character of Na-MMT. In SEM analyses, we found lots of Na-MMT precipitated on the surface of CF and HF. Therefore, their moisture contents increased significantly. But for LF, the moisture content changed a little, probably because the silicate filler was well encapsulated by the hydrophobic LF.

After modifying, it was apparent that OMMT restricted the hygroscopicities of HF and LF samples, especially HF with final moisture content of 46.09%, which showed 4% and 7% loss of weight compared to neat and Na-MMT modified HF. Seethamraju et al.[41] added OMMT into Surlyn matrix by using a copolymer of vinyl alcohol and ethylene as dispersant and found that high dispersion and interaction between OMMT and polymer matrix could reduce the water vapor permeability of the composite. Therefore, the results of decreased moisture content could be also associated with the intercalated or exfoliated structure of OMMT in HF and LF, causing barrier effect on moisture adsorption. However, the moisture content of OMMT modified CF sample was higher than neat CF at each stage though these values were lower than Na-MMT treated CF. This might be explained by agglomeration of OMMT on CF surface, which could not reduce the moisture content. Adversely, the OMMT itself could adsorb some moisture through capillary at inner space of OMMT.

Nanoindentation

The nanoindentation results for the mechanical properties of neat, Na-MMT, and OMMT modified NF components are summarized in Table 1. Irrespective of deviations, the modulus of elasticity of Na-MMT treated CF, HF, and LF were slightly increased from 1.27 GPa to 1.65 GPa, 0.34 GPa to 0.37 GPa and 2.33 GPa to 2.48 GPa, respectively. Simultaneously, the hardness increased from 0.12 GPa to 0.14 GPa, 0.03 GPa to 0.04 GPa and 0.21 GPa to 0.24 GPa, respectively, suggesting little influence of Na-MMT treatment on mechanical properties of NF components. This was because Na-MMT did not well disperse into NF components but gathered on their surfaces

based on SEM and TEM results. OMMT modified HF and LF exhibited higher values of modulus of elasticity and hardness than neat and Na-MMT treated HF and LF, especially the LF group with relative high modulus of elasticity and hardness values of 4.13 GPa and 0.54 GPa, which indicated the intercalated or exfoliated silicate layers in HF and LF significantly improve the mechanical properties of HF and LF. Gurunathan et al.[42] added OMMT into polyurethane matrix and tested the tensile property of the composite. In their study, with the addition of clay from 0 to 2 wt%, the Young's modulus of composites increased from 22.3 MPa to 134.8 MPa. Our results were consistent with theirs. These enhancements of mechanical properties are associated with the interfacial interaction between OMMT and NF polymer. The strong interaction bond allowed load transfer capability from the NF polymer to the stiff OMMT and then reduced the slippage of NF molecular chains during compression, thus resulting in improvements in mechanical properties. The modulus of elasticity and hardness of OMMT modified CF were 1.88 GPa and 0.16 GPa, which showed little change compared with neat or Na-MMT treated CF. Confirmed by the SEM and TEM analyses, lots of OMMT gathered on the surface of CF. Consequently, the filler–filler interaction was effective over the filler–polymer interaction, which was helpless to the improvements of mechanical properties.

^{13}C NMR analysis

The ^{13}C NMR analysis was carried out to further understand the interaction mechanisms between OMMT and NF components. The spectra of the neat, Na-MMT treated, and OMMT modified NF components are shown in Fig.6. The chemical shift assignments of spectra of NF components and OMMT were made on the basis of literature data.[40, 43-49] Overall, CF, HF and LF gave characteristic signals in the ^{13}C NMR spectra shown in Fig.6a, 6b, and 6c, respectively. In these figures, the curves of Na-MMT treated NFs were much similar to neat NFs, showing no reactions were found between Na-MMT and NFs.

Cellulose. As shown in Fig.6a, peaks assigned to the carbons in the cellulose backbone at 103.87 (C1), 87.80 (C4 of crystalline CF), 83.04 (C4 of amorphous CF), 73.71, 70.89 (C2, C3, C5), 64.13 (C6 of crystalline CF), and 61.40 (C6 of amorphous CF) ppm, respectively,[43] were evidently detected in both neat CF and OMMT modified CF. Besides, two small signals at 20.36 and 13.50 ppm, which were related to the $-CH_3$ groups in acetyl groups of hemicelluloses residues were observed in the neat CF sample.

After modifying with OMMT, a new small peak at 28.79 ppm existed, which was associated with the long alkyl chains from C2 to C10 of OMMT.[44] Besides, the peak at 28.79 ppm shift to 22.08 ppm due to the C11 methylene group of OMMT overlapped the $-CH_3$ groups of HF or some reactions happened. These two peaks suggested the existence of OMMT in CF. However, it was not bonded on the molecular chains of CF because no extra changes were found.

Hemicelluloses. Fig.5b revealed there were four important groups in neat HF, namely, (1,4)-β-D-Xylp, (1,4)-α-D-Xylp, O-acetyl-β-D-Xylp, and 4-O-methyl-α-D-GlcpA groups. Peaks detected at 101.26 (C1), 72.77 (C2, C3 and C4), and 63.65 (C6) ppm were characteristics of D-Xylp units.[43] The signals at 91.69 and 91.69 ppm proved that the linkage of HF had both (1,4)-β-D-Xylp and (1,4)-α-D-Xylp units.[45] Besides, some weak peaks were found at 103.07 and 99.55 ppm, indicating the a few amounts of O-acetyl-β-D-Xylp units on position of C3 and C2, respectively.[43] Besides, the peak at 58.46 ppm corresponding to C4 of 4-O-methyl-α-D-GlcpA was also detected in the spectra analysis, which was linked on position of C3 and C2 of the xylan bone.[40] Based on the NMR results, the structure of neat HF before modifying with OMMT mainly consisted of both(1,4)-β and (1,4)-α-D-Xylp with some O-acetyl groups on position of C3 and C2, and 4-O-methyl-glucuronic acid groups linked on position C3 and C2 of the xylan bone.

Compared with neat HF, most of the signals in OMMT modified HF sample were detected. However, there were four differences: (1) intensity of peaks at 96.48 and 63.65 ppm decreased, indicating breakage of short-ranged (1,4)-β-D-Xylp linkage and open-ring of D-Xylp units; (2) signals at 103.07 and 99.55 ppm disappeared, which was caused by the removal of unstable O-acetyl units from the HF backbone; (3) peak at 58.46 ppm disappeared and a new small new peak at 81.03 ppm was found, suggesting the reaction of 4-O-methyl-α-D-GlcpA and formation of small amount of 4-O-methyl-α-D-GalUA during hydrolyzation;[46] (4) the peak at 101.26 shifted to a higher chemical shift at 102.17 ppm, due to overlapping of formed $COON(CH_3)_2(C_{12}H_{26})_2$ between generated –COOH and cationic chains in OMMT. Thus, some HF molecular chains entered into the gallery of OMMT, enlarging the interlayer distance of OMMT. Scheme 1 shows the interaction mechanism of OMMT with HF, and can be described as followed: numbers of short-ranged (1,4)-β-D-Xylp linkage of HF broke, liberating more end hydroxyl groups. Under DDAC alkaline condition, the end hydroxyl groups of HF became an open-ring structure and then oxidized to carboxyl groups. Simultaneously, some unstable units removed from the HF main chains. The carboxyl groups were easily ionized and reacted with ammonium cationic chains in OMMT, thus to enlarge the interlayer distance of OMMT. It should be mentioned that the differences between neat HF and OMMT modified HF were ambiguous due to the low concentration of OMMT (0.5%).

Lignin. The structures of LF were more complicated than CF and HF. As shown in Fig.5c, the spectrum of LF can be divided into several regions: (1) broad region between 155 and 110 ppm was specific for aromatic carbons of LF; (2) small peaks from 90 to 60 ppm were β-O-4 linkages for LF benzene units; (3) signal at 55 ppm was ascribed to the C-H in methoxyl side groups of LF; (4) signals around 28 ppm were associated with alkyl chains of LF,[47-49] in which, the regions of 155-110 and 90-60 ppm were used to characterize for structures of neat LF. Besides, because the separation of LF was carried out by ball-milling process, some polysaccharide of HF may remain. So some small signals at 174 ppm and 22 ppm assigned to the carboxylic groups and methyl groups of the acetyl functions of hemicelluloses residues were found.

After modifying with OMMT, signals at 132 and 128 ppm related to the hydroxybenzoate substructures and hydroxycinnamyl alcohol end groups disappeared and a new

strong peak at 130 ppm appeared. Thus, the phenolic carboxyl groups and phenolic hydroxyl groups of LF were reacted with OMMT. Besides, the signal at 73 ppm (β-O-4 linkage) decreased, suggesting the cleavage of lignin, which made more phenolic hydroxyl groups available. Moreover, the signal at 170 ppm appeared which was induced by the reactions between carboxyl groups and the ammonium salt. Thus, the reactions between LF and OMMT can be concluded as follows (shown in scheme 2): During modification, some molecular chains of LF broke and left more phenolic hydroxyl groups and carboxyl groups available, which reacted with the ammonium cationic chains of OMMT. Therefore, the OMMT layers were bonded onto LF. Owing to the net-work structures of LF, the OMMT layers exfoliated into individual sheets and uniformly dispersed into LF matrix.

Conclusions

For different NF components, although their different morphologies might have influence on MMT dispersion, a more important factor should be the different chemical structures of NFs. OMMT mainly reacted with the amorphous constituents of NF cell wall, namely, it can be intercalated with HF while completely exfoliated in LF. The reactions were formed basically on end carboxyl or phenolic hydroxyl groups of HF and LF chain. Due to the successful reactions, decrease of moisture contents and increase of mechanical properties were found both in OMMT modified HF and LF samples. However, no reactions were found between OMMT and CF, a large amount of OMMT just physically absorbed and attached on CF surface, which had negative effect on reduction of moisture adsorption behaviour and little effect to the improvements in mechanical properties.

Acknowledgements

This study was financially supported by the National Natural Science Foundation of China (No. 31170524).

References

1. D. Roy, M. Semsarilar, J. T. Guthrie and S. Perrier, *Chem. Soc. Rev.*, 2009, **38**, 2046-2064.
2. M. N. Mirvakili, S. G. Hatzikiriakos and P. Englezos, *ACS Appl. Mater. Interfaces*, 2013, **5**, 9057-9066.
3. J. Song, Aimin Tang, T. Liu and J. Wang, *Nanoscale*, 2013, **5**, 2482-2490.
4. P. Wambua, J. Ivens and I. Verpoest, *Compos. Sci. Technol.*, 2003, **63**, 1259-1264.
5. M. R. Pelaez-Samaniego, V. Yadama, E. Lowell and R. Espinoza-Herrera, *Wood Sci. Technol.*, 2013, **47**, 1285-1319.
6. A. K. Bledzki and J. Gassan, *Prog. Polym. Sci.*, 1999, **24**, 221-274.
7. M. Ibrahim, *Cellulose*, 2002, **9**, 337-349.
8. F. Peng, P. Peng, F. Xu and R. Sun, *Biotechnol. Adv.*, 2012, **30**, 879-903.
9. T. Saito, R. H. Brown, M. A. Hunt, D. L. Pickel, J. M. Pickel, J. M. Messman, F. S. Baker, M. Keller and A. K. Naskar, *Green Chem.*, 2012, **14**, 3295-3303.
10. R. Liu, Y. Peng and J. Cao, *Compos. Sci. Technol.*, 2014, **103**, 1-7.
11. C. Zhou, Z. Shen, L. Liu and S. Liu, *J. Mater. Chem.*, 2011, **21**, 15132-15153.
12. C. Aulin, G. Salazar-Alvarez and T. Lindström, *Nanoscale*, 2012, **4**, 6622-6628.
13. D. L. Schrijvers, F. Leroux, V. Verney and M. K. Patel, *Green Chem.*, 2014, **16**, 4969-4984.
14. S. P. Kumar, S. Takamori, H. Araki and S. Kuroda, RSC Adv., 2015, **5**, 34109-34116.
15. F. O. Cheng, T. H. Mong and R. L. Jia, *J. Polym. Res.*, 2003, **10**, 127-132.
16. J. F. Timmerman, B. S. Hayes, J. C. Seferis, *Compos. Sci. Technol.*, 2002, **62**, 1249-1258.
17. N. A. Siddiqui, R. S. C. Woo, J. K. Kim, C. C. K. Leung, A. Munir, *Comps. Part A-Appl. Sci.*, 2007, **38**, 449-460.
18. P. Chen, L. Jiang and D. Han, *Small*, 2011, **7**, 2825-2835.
19. J. Wang, Q. Cheng, L. Lin, L. Chen and L. Jiang, *Nanoscale*, 2013, **14**, 6356-6362.
20. H. M. Park, X. Liang, A. K. Mohanty, M. Misra and L. T. Drzal. *Macromolecules*, 2004, **37**, 9076-9082.
21. L. A. Utracki, M. Sepehr and E. Boccaleri, *Polym. Advan. Technol.*, 2007, **18**, 1-37.
22. R. Liu, S. Luo, J. Cao and Y. Peng, *Compos. Part A-Appl. Sci.*, 2013, **51**, 33-42.
23. R. Liu, Y. Peng and J. Cao, *Ind. Crop. Prod.*, 2014, **62**, 387-394.
24. P. Mäki-Arvela, T. Salmi, B. Holmbom, S. Willför and D. Y. Murzin, *Chem. Rev.*, 2011, **111**, 5638-5666.
25. TAPPI Test Method T 203 om-93. Atlanta, Georgia, USA: TAPPI, 1994.
26. K. M. Holtman, H. M. Cheng, H. Jameel, J. F. Kadla, *J. Wood Chem. Technol.*, 2006, **26**, 21-34.
27. C. Xing, S. Wang, G. M. Pharr and L. H. Groom, *Holzforschung*, 2008, **62**, 230-236.
28. H. Zhao, J. H. Kwak, Z. C. Zhang, H. M. Brown, B. W. Arey and J. E. Holladay, *Carbohyd. Polym.*, 2007, **68**, 235-241.
29. P. D. Carà, M. Pagliaro, A. Elmekawy, D. R. Brown, P Verschuren, N. R. Shiju and G. Rothenberg, *Catal. Sci. Technol.*, 2013, **3**, 2057-2061.
30. H. M. Park, W. K. Lee, C. Y. Park, W. J. Cho and C. S. Ha, *J. Mater. Sci.*, 2003, **38**, 909-915.
31. H. T. Liao and C. S. Wu, *Macromol. Mater. Eng.*, 2005, **290**, 695-703.
32. M. Kačuráková, A. Ebringerová, J. Hirsch and Z. Hromádková, *J. Sci. Food Agric.*, 1994, **66**, 423-427.
33. D. K. Shen, S. Gu and A. V. Bridgwater, *J. Anal. Appl. Pyrol.*, 2010, **87**, 199-206.
34. O. Derkacheva and D. Sukhov, *Macromol. Symp.*, 2008, **265**, 61-68.
35. X. Jiang, J. Gu, X. Tian, Y. Li and D. Huang, *Bioresource Technol.*, 2012, **104**, 473-479.
36. F. Peng, J. Bian, J. Ren, P. Peng, F. Xu and R. Sun, *Biomass Bioenerg.*, 2012, **39**, 20-30.
37. O. Gordobil, I. Egüés, I. Urruzola and J.l Labidi, *Carbohyd. Polym.*, 2014, **112**, 56-62.
38. W. Xue, H. He, J. Zhu and P. Yuan, *Spectrochim. Acta A*, 2007, **67**, 1030-1036.
39. L. Bromberg, C. M. Straut, A. Centrone, E. Wilusz and T. A. Hatton, *ACS Appl. Mater. Interfaces*, 2011, **3**, 1479-1484.
40. Y. Luo, S. Shen, J. Luo, X Wang and R. Sun, *Nanoscale*, 2015, **7**, 690-700.
41. S. Seethamraju, P. C. Ramamurthy and G. Madras, *RSC Adv.*, 2014, **4**, 11176-11187.
42. T. Gurunathan, S. Mhanty and S. K. Nayak, *RSC Adv.*, 2015, **5**, 11524-11533.
43. H. Kim and J. Ralph, Org. *Biomol. Chem.*, 2010, **8**, 576-591.
44. M. A. Osman, M. Ploetze and P. Skrabal, *J. Phy. Chem. B*, 2004, **108**, 2580-2588.
45. T. Yuan, S. Sun, F. Xu and R. Sun, *J. Agric. Food Chem.*, 2011, **59**, 10604-10614.
46. H. Tang, P. S. Belton, A. Ng and P. Ryden, *J. Agric. Food Chem.*, 1999, **47**, 510-517.
47. H. Yuzawa, M. Aoki, H. Itoh and H. Yoshida, *J. Phys. Chem. Lett.*, 2011, **2**, 1868-1873.
48. X. Du, G. Gellerstedt and J. Li, *Plant J.*, 2013, **74**, 328-338.
49. R. Kumar, F. Hu, P. Sannigrahi, S. Jung, A. J. Ragauskas and C. E. Wyman, *Biotechnol. Bioeng.*, 2013, **110**, 737-753.

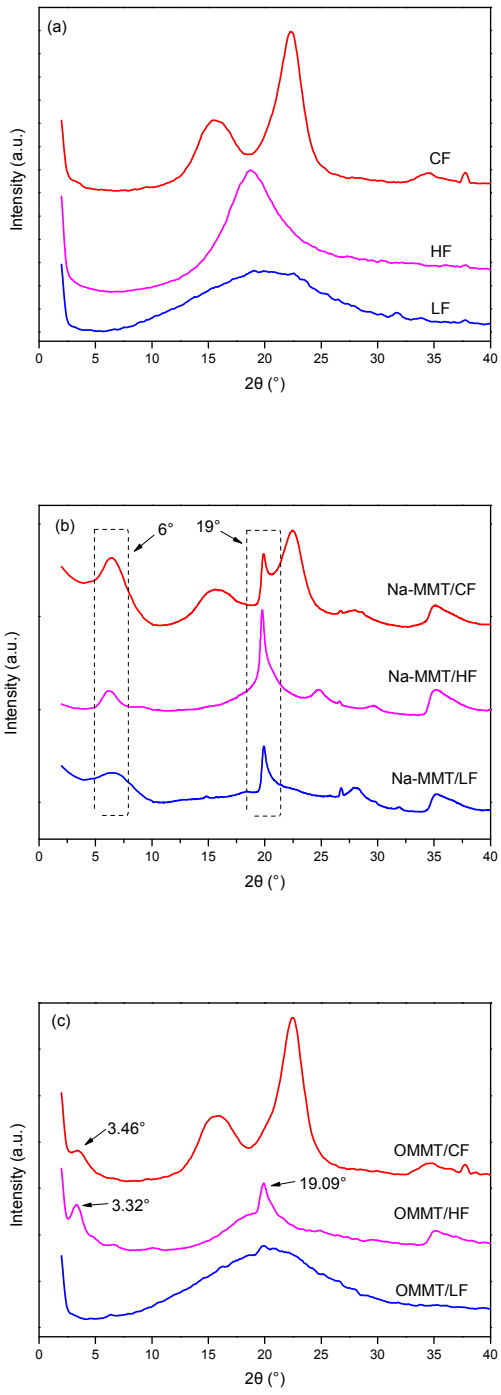

Fig.1 XRD patterns of neat (a), Na-MMT (b) and OMMT modified (c) NF components

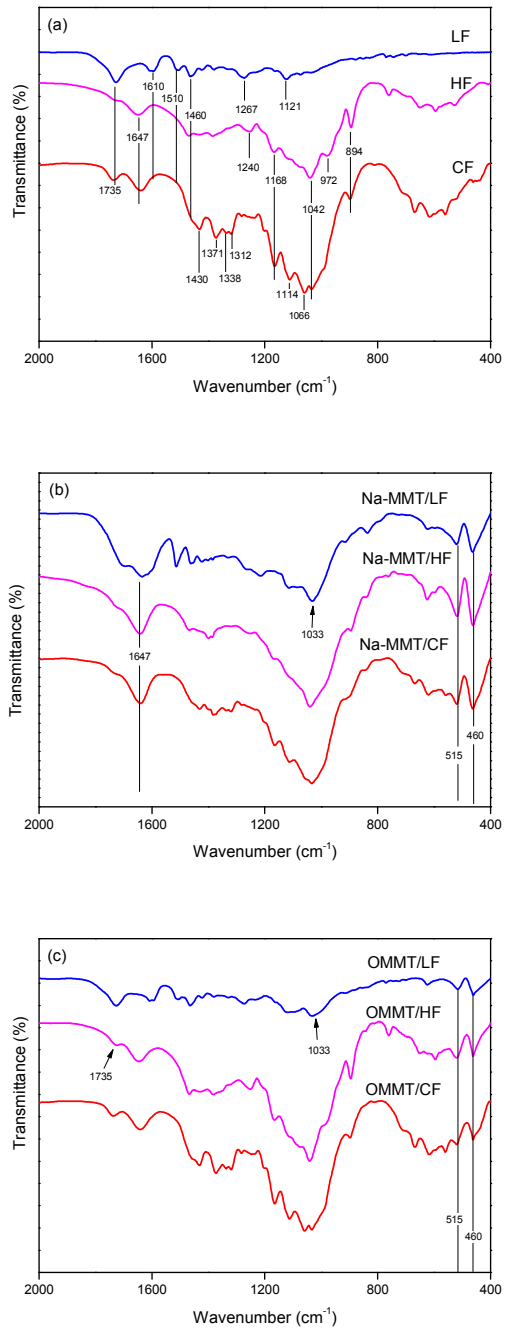

Fig.2 FTIR spectra of neat (a), Na-MMT (b) and OMMT modified (c) NF components

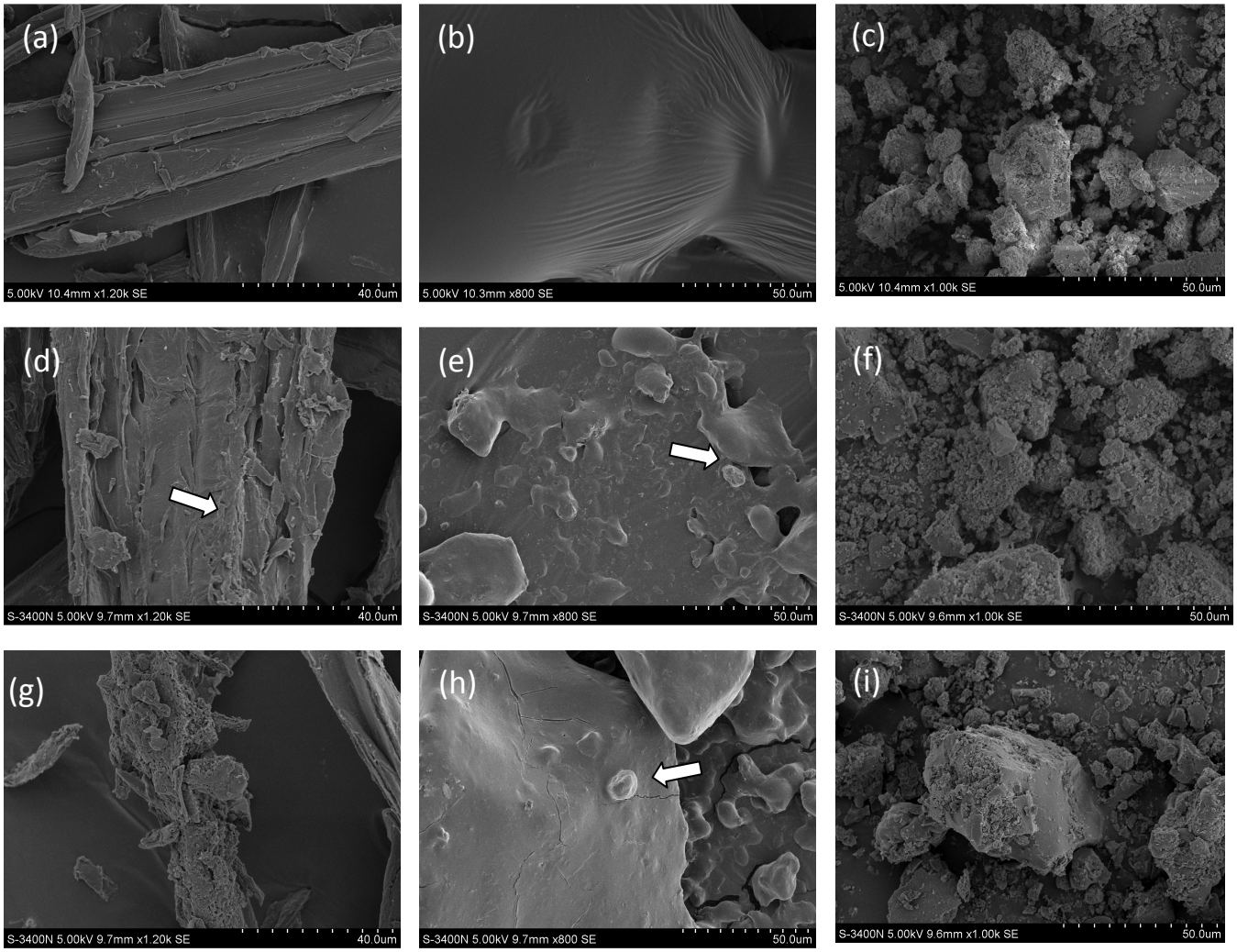

Fig.3 SEM images of neat (a-c), Na-MMT (d-f) and OMMT (g-i) modified NF components: CF (a, d, g), HF (b, e, h), LF (c, f, i)

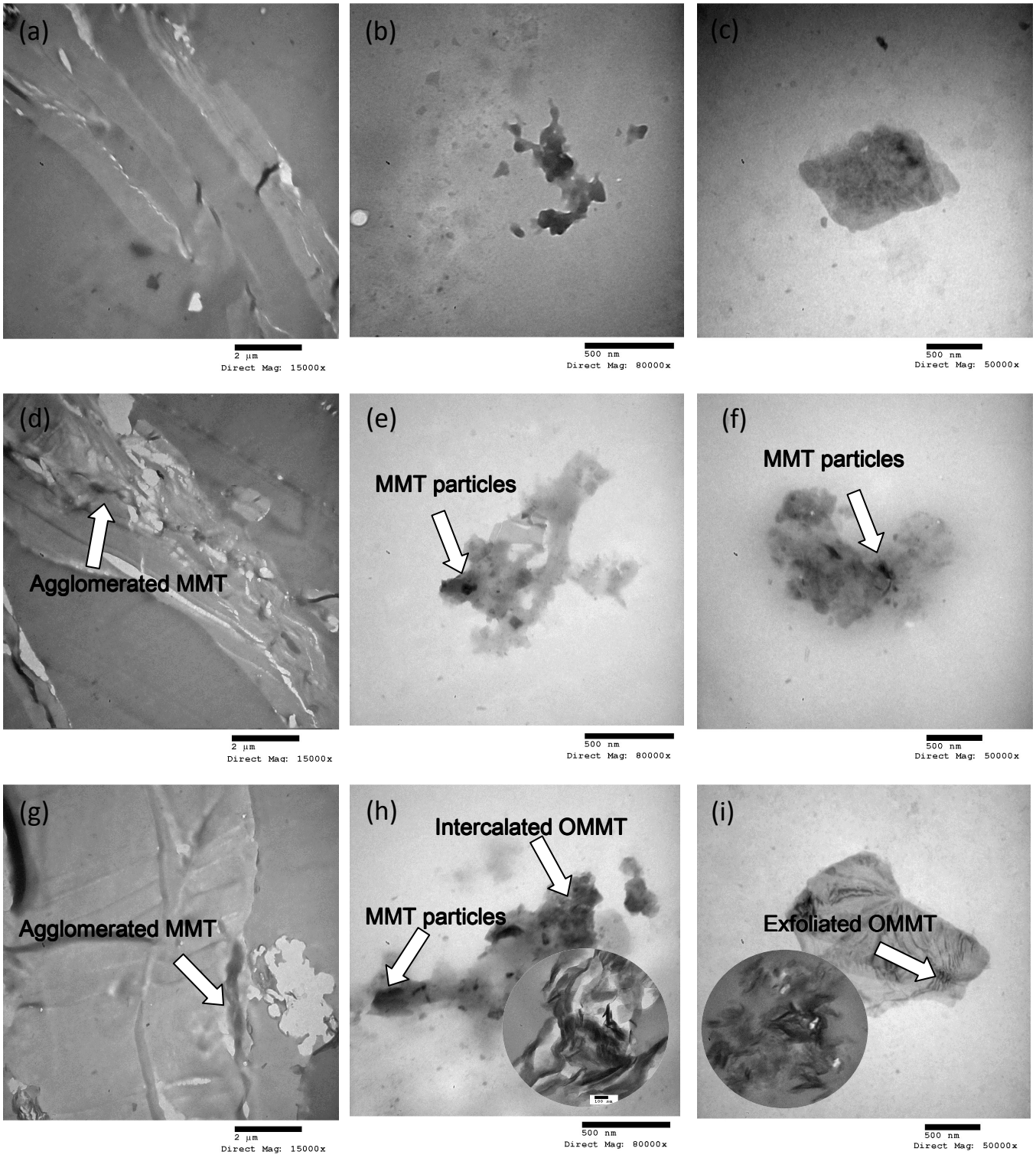

Fig.4 TEM images of neat (a~c), Na-MMT (d~f) and OMMT (g~i) modified NF components: CF (a, d, g), HF (b, e, h), LF (c, f, i)

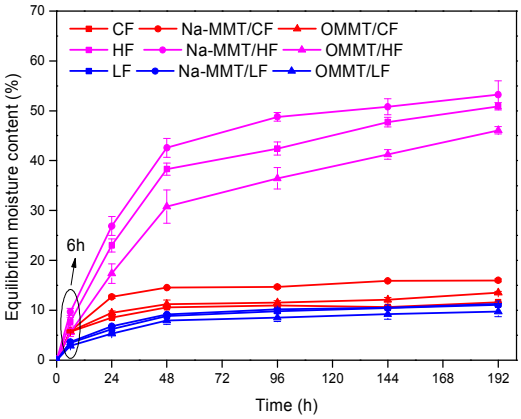

Fig.5 Equilibrium moisture contents of neat, Na-MMT and OMMT modified NF components

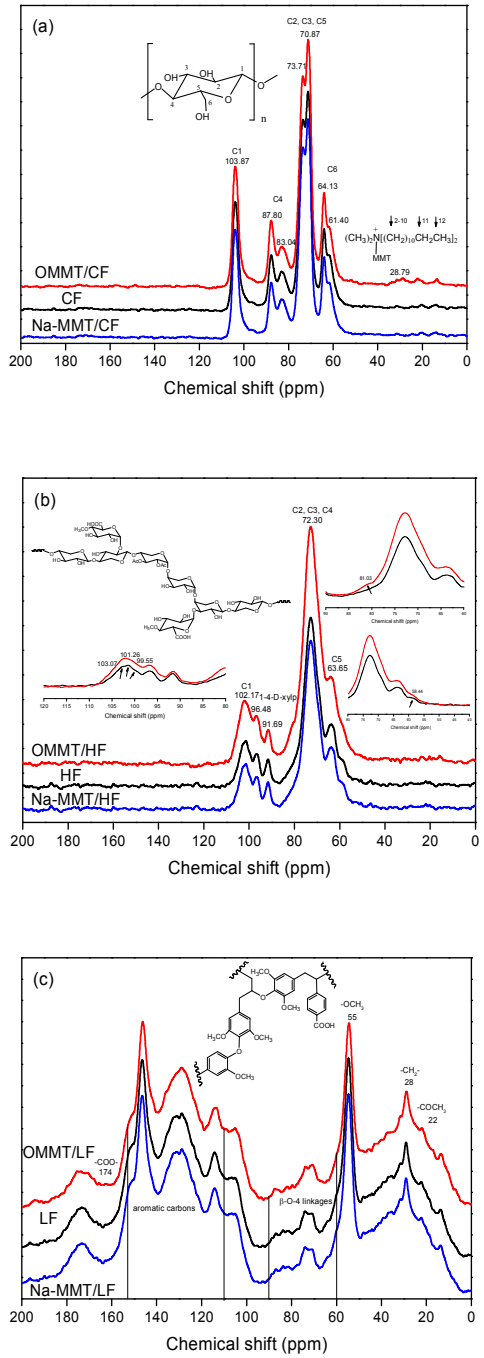

Fig.6 ^{13}C NMR spectra of neat, Na-MMT treated and OMMT modified CF (a), HF (b), and LF (c)

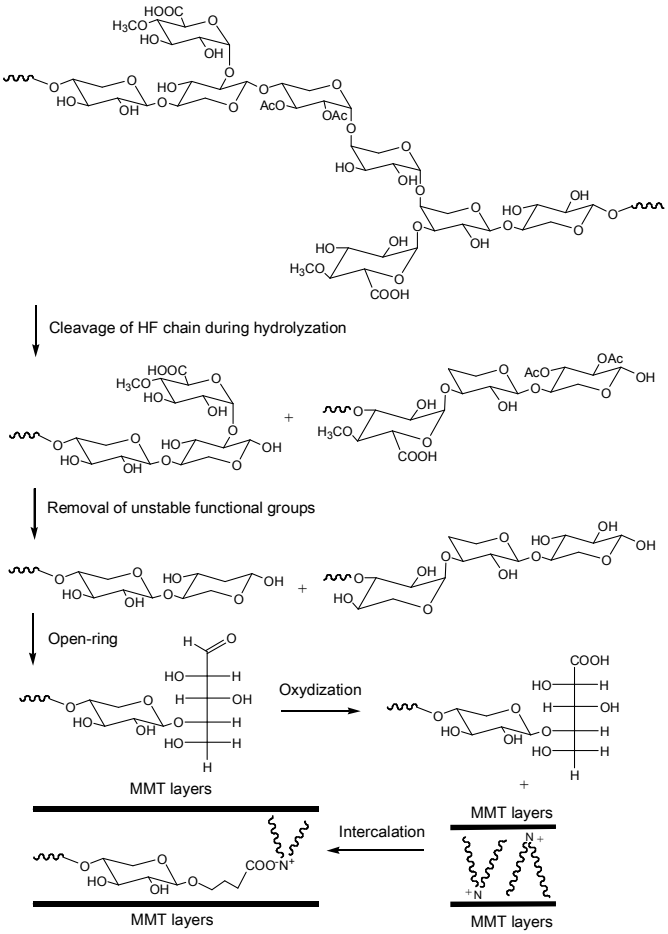

Scheme 1 Suggested formation of HF intercalated OMMT structures

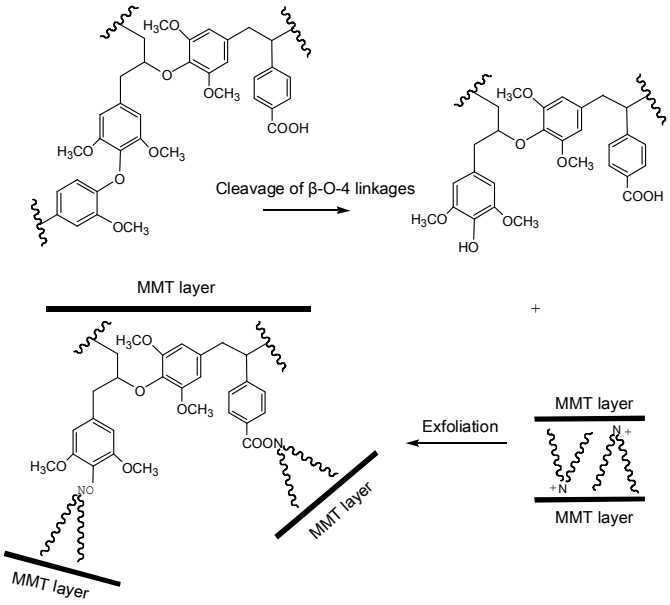

Scheme 2 Suggested formation of LF exfoliated OMMT structures

Table 1 Mechanical properties of neat, Na-MMT and OMMT modified NF

Labels	Mechanical properties	
	Modulus of elasticity (GPa)	Hardness (GPa)
CF	1.27 (0.06)	0.12 (0.04)
Na-MMT/CF	1.65 (0.12)	0.14 (0.01)
OMMT/CF	1.88 (0.33)	0.16 (0.03)
HF	0.34 (0.04)	0.03 (0.01)
Na-MMT/HF	0.37 (0.17)	0.04 (0.01)
OMMT/HF	1.87 (0.12)	0.10 (0.02)
LF	2.33 (0.44)	0.21 (0.08)
Na-MMT/LF	2.48 (0.53)	0.24 (0.04)
OMMT/LF	4.13 (0.32)	0.54 (0.08)

Note: Values in parentheses are standard deviations of 10 replicates.